Carbon nanotubes supported N-promoted Pd-based catalysts for acetylene hydrochlorination

Lu Wang[1,2,*#], Shahid Ali[1#], Jianxin Si[1], Lizhen Lian[1], Haijun Yan[1], Jide Wang[1] and Lida Ma[2]
[1]Key laboratory of oil and gas fine chemicals of education and xinjiang uygur autonomous region, College of chemical engineering, Xinjiang university, Urumqi, Xinjiang, China.
[2]Xinjiang De'an environmental protection technology incorporated company, Urumqi, Xinjiang, China.

Abstract. A novel N-promoted carbon nanotubes (CNT) supported Pd catalyst (PANI/CNT-Pd) was prepared by the ultrasonic-assisted impregnation method and applied in the acetylene hydrochlorination reaction successfully. Compared with the Pd-CNT catalyst, the PANI/CNT-Pd catalyst exhibited the enhanced catalytic performance with more than 91.6% acetylene conversion and 99.6% vinyl chloride selectivity during 20 h at T = 160 °C, GHSV(C_2H_2) = 120 h^{-1} and V(HCl) : V(C_2H_2) = 1.5. It is suggested that PANI species contained N elements have been deposited on the CNT surface and they display the critical role on the enhanced catalytic performance of PANI/CNT-Pd catalysts correlated with the less palladium loss and the carbon deposition.

1. Introduction

Due to the increasing petroleum prices and abundant coal resources in China, the coal-based acetylene hydrochlorination is the optimal chemical reaction for the manufacture of vinyl chloride monomer (VCM), which is a major raw material for polyvinyl chloride (PVC)[1]. At present, the HgCl2 supported on active carbon (AC) catalyst is widely carried out in industrial PVC production with high Hg pollutions and shortages in Hg resource, leading to severe environmental and economic problems, restricting the PVC sustainable development[2-3]. Therefore, it is highly urgent to search for non-mercury catalysts to replace mercuric chloride in the acetylene hydrochlorination reaction.

In the last decades, precious metals-based (Au, Pt, Pd, Ru, etc) catalysts were considered as the most potential metal catalyst applied for acetylene hydrochlorination[4-7]. However, the activities and stabilities of the precious metals-based catalysts were decreased rapidly for the carbon deposition, the changes of metal phase (including reduction, sintering and loss of metals) and other reasons, largely limiting their application for industrial acetylene hydrochlorination[1-7]. So it remains attractive to research the modification strategies for improving the catalytic performance of precious metals-based catalysts for acetylene hydrochlorination, such as other meatal modification (K, Cu, La, Ce, Bi, etc)[8-12], heteroatom modification (N, P, S, B, etc) of support[13-16], ionic liquid modification[17-18], preparation method exploration[6,8,15-16,19-20]. It is suggested that appropriate modification strategies can stabilize the catalytic active component, promote the active component dispersion, enhance the chemisorption of reactants (hydrogen chloride or acetylene), retard the active component loss and inhibit the carbon deposition[4-19]. In addition, the nature of the catalyst support has been focused and it is considered that the suitable carrier is good to the reactivity promotion for acetylene hydrochlorination[19]. So many other carriers (zeolites, Al_2O_3, SiO_2, etc) have been used for acetylene hydrochlorination as well as AC[21-23].

Carbon nanotubes (CNT) are generally considered as an extremely promising material for their high mechanical strength, large surface area, excellent electrical conductivity and good adsorption performance[24-26]. It is reported that nitrogen-doped carbon nanotubes can improve electron-transport quality and electrical properties[27-29] and CNT incorporated with conducting polymers (polyaniline, polypyrrole, etc) have been attracted much attention in a wide variety of applications such as fuel cells, catalysis, gas sensors and polymers, owing to their simple synthesis, outstanding dispersibility and environmental stability recently[27-32]. In our previous work, palladium-based catalysts with excellent activity were considered as the potential mercury-free catalysts for acetylene hydrochlorination, but non-ideal stability still needs improvements[6,8,16,21,30]. In this work, polyaniline (PANI) as the main nitrogen source grafted onto the surface of carbon nanotubes were prepared by chemical oxidation polymerization method and palladium supported on PANI/CNT catalysts (PANI/CNT-Pd) were achieved by the ultrasonic-assisted impregnation method, applied for acetylene hydrochlorination successfully. The catalytic performance and physicochemical properties of PANI/CNT-Pd catalysts were explored, and the possible reasons for the catalyst deactivation were discussed.

* Corresponding author: wanglu_4951@163.com
#The two authors contributed equally to this work.

2.Experimental

2.1.Preparation of the catalysts

PANI/CNT composites were prepared by chemical oxidation polymerization method[30,33]. A volume of 100 mL HCl solution (2 M) containing CNT (2.0 g) suspension was sonicated at room temperature for about 0.5 h, and then mixed with 2 mL aniline monomer (CP, N98%, 4 mL). Ferrous sulfate solution (5%,1 mL) was added followed by the addition of ammonium persulfate (CP, N98%, 0.5 g mL-1) which served as the oxidant. The reaction mixture was constantly stirred in an ice bath (temperature range of 0-5 °C) for 1 h and then reacted at room temperature for 3 h. The dark green precipitates (PANI species) were filtered and washed with distilled water/ethanol until the filtrate became colorless. After drying at 80 °C for 10 h, the PANI/CNT composites with the mass ratio of 30%, 40%, 60%, 80% PANI species were obtained and labeled as 3PANI/CNT, 4PANI/CNT, 6PANI/CNT, 8PANI/CNT, respectively.

The catalysts were all prepared by the ultrasonic-assisted impregnation method[15,16]. PANI/CNT composites were dried at 100 °C for 2 h for removing the adsorbed water before the H2PdCl4 solution was added dropwise to the PANI/CNT carriers (3.0 g) with continuous stirring at normal temperature. Then the mixture was impregnated with ultrasonic treatment for 1 h and stored at room temperature overnight. Finally, the obtained samples were dried at 90 °C for 10 h and recorded as PANI/CNT-Pd catalysts. The serial PANI/CNT-Pd catalysts were named in terms of the PANI/CNT carriers, which were designated as 3PANI/CNT-Pd, 4PANI/CNT-Pd, 6PANI/CNT-Pd and 8PANI/CNT-Pd, respectively. For comparison, the Pd-CNT catalyst was prepared using the similar method described above without PANI. Additionally, the Pd loading of all catalysts was kept 0.5 wt%.

2.2.Catalyst characterization

Fourier transform infrared spectrometer (FTIR) was recorded at 364 scans per spectrum at 4 cm-1 resolution, using EQUINOX-55 (Bruker Company, Germany) machine. The relative ingredients and microtopography of catalysts were recorded by an energy dispersive spectrometer (EDS) analyzer attached to a LEO1450VP scanning electron microscope (SEM). The real content of palladium species was detected using an inductively coupled plasma instrument (Agilent ICP-OES730). X-ray powder diffraction (XRD) data were collected on M18XHF22-SRA diffractometer using Cu-Kα radiation (scanning range 2θ: 10-80°) at 50 kV and 100 mA. Brunauer-Emmett-Teller (BET) surface areas and pore parameters were measured by Quantachrome autosorb iQ2 equipment.

2.3 Catalyst measurement

The catalytic test for acetylene hydrochlorination was carried out in a fixed bed with a 10-mm-diameter quartz microreactor operating just above atmospheric pressure. N2 flow (15 mL min-1) via calibrated mass flow controllers in a heated glass reactor and then hydrochloride at a flow rate of 15 mL min-1 passed through the reactor to activate the catalyst. Hydrochloride (12.8 mL min-1) and acetylene (8.5 mL min-1) were fed through a mixing vessel containing catalyst (3.0 g) under the reaction conditions (T = 160 °C, a C2H2 gas hourly space velocity (GHSV) = 120 h-1 and VHCl: VC2H2 = 1.5). The exit gas mixture from the reactor was passed through an absorption bottle filled with sodium hydroxide solution and then analyzed acetylene conversion and VCM selectivity by gas chromatography (GC 2010, Shimadzu).

3. Results and discussion

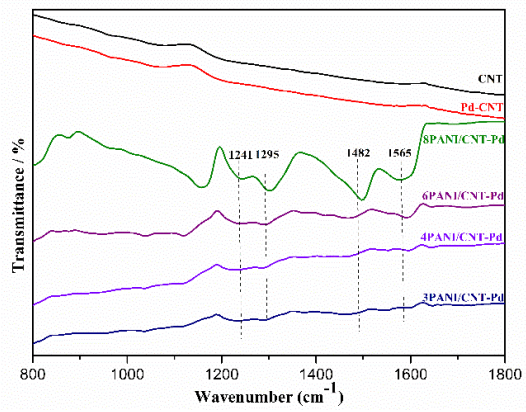

Fig.1. FTIR spectra of CNT and Pd-based catalysts

FTIR spectra of the CNT and Pd-based catalysts were presented in Fig 1. Like graphite, the FTIR spectrum of pristine CNT carrier and the Pd-CNT catalyst all had extremely low infrared absorption intensities and it is suggested that there are no obvious changes of functional groups on the Pd-CNT catalyst surface after loading Pd active components. For PANI/CNT-Pd composites, the almost identical characteristic bands situated at 1241 cm-1, 1295 cm-1, 1482 cm-1 and 1565 cm-1 were attributed to C=N stretching vibrations, stretching of C-N secondary aromatic amine, benzenoid stretching vibration, a quinoid-ring vibration[34]. Compared with Pd-CNT, some main bands of PANI were observed in PANI/CNT-Pd nanocomposites, though they shifted to a lower wavenumber as a result of the additional π-π conjugated interaction between the benzene ring of PANI and the graphite-structured CNT, indicating an interaction between CNT and PANI[34].

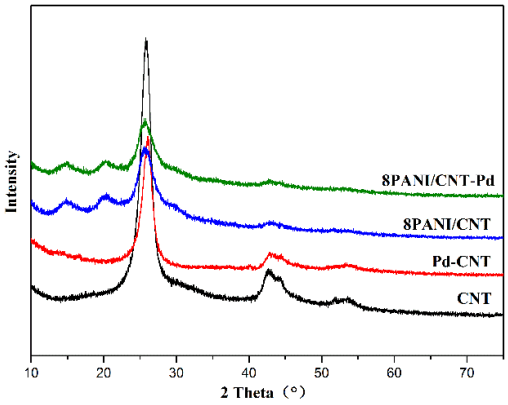

Fig.2. XRD patterns of CNT and Pd-based catalysts

Fig 2 displayed the X-ray diffraction data for the CNT, PANI-CNT composites and fresh Pd-CNT and 8PANI/CNT-Pd catalysts. The diffraction peaks of the pure CNT at the 2θ angle of 25.9° and 42.5° were assigned to the typical peak of the (002) and (100) of the graphite-like structure in CNT, respectively[35-36]. In the XRD patterns of PANI/CNT composites, the diffraction peaks were detected at 2θ around 14.9°, 20.3° and 25.7°, which corresponding to (011), (020) and (200) crystal planes of PANI, respectively[37]. The fact that XRD patterns of the 8PANI/CNT-Pd catalyst were similar to that of the 8PANI/CNT composites and no visible Pd species were detected in the fresh 8PANI/CNT-Pd catalyst, in spite of adding greater Pd concentration, indicating the Pd active component remained highly dispersed on the surface of the carrier[6,8,16,30,33]. In addition, it is revealed that the typical peak intensities of the (002) graphite-like structure (2θ at around 25.9°) weakened in 8PANI/CNT composites and turned into the (200) crystal planes of PANI (2θ at around 25.7°). From a structural point of view, it was clear that part of the CNT carrier had fully interacted with PANI molecules, accorded with the FTIR results (Fig 1). Meanwhile, the peak centered at 2θ around 25.0° could be attributed to periodicity perpendicular to the polymer chains[38]. This result also indicated that the CNT doped PANI was crystalline polymer and no additional crystalline orders had been introduced.

The morphologies of the CNT and PANI/CNT composites with various PANI contents have been examined by scanning electron microscopy (SEM) shown in Fig 3. As shown in Fig 3a, the pure CNT was entangled and interconnected. Initially, as the mass ratio of PANI is 30% (3PANI/CNT), PANI is glossily coated onto the surface of the CNT carrier (Fig 3b). When the mass ratio of PANI species increased, the morphologies of the PANI/CNT composites were changeable continually (Fig 3c and Fig 3d). As the mass ratio of PANI species reached to 80% (8PANI/CNT), the PANI layer becomes rougher, which showed a considerable rough surface deposit coated the CNT surface, attributed to the fresh PANI deposition (Fig 3d). This indicated that the morphological structure of the PANI/CNT composites was dependent on the mass ratio of PANI species.

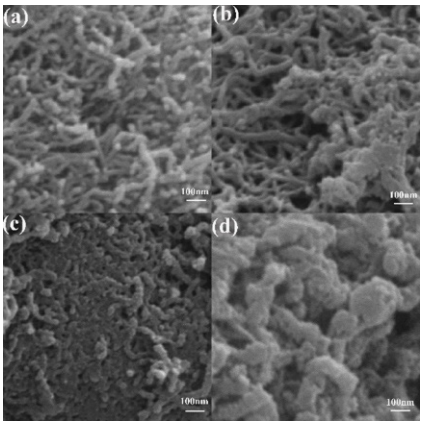

Fig.3. SEM images of CNTs and PANI/CNTs composites. (a) CNT; (b) 3PANI/CNT; (c) 6PANI/CNT; (d) 8PANI/CNT.

Table 1. Elemental composition of the catalyst record by EDS.

Sample	Relative elemental compositions(wt%)					
	C	O	N	Cl	S	Pd
CNT	91.42	8.58	0	0	0	0
8PANI/CNT	81.89	0.11	12.01	5.01	0.98	0
Fresh Pd-CNT	97.54	0.51	0	0.93	0	1.02
Used Pd-CNT	98.38	0.21	0	1.10	0	0.31
Fresh 8PANI/CNT-Pd	64.71	1.14	24.50	6.96	1.51	1.18
Used 8PANI/CNT-Pd	72.91	0.21	15.11	10.59	0.47	0.62

Table 2 The total Pd content of the Pd-CNT and 8PANI/CNT-Pd catalysts recorded by ICP.

Catalysts	Total Pd (wt%)		Loss ratio of Pd (%)
	Fresh	Used	
Pd-CNT	0.87	0.43	50.6
8PANI/CNT-Pd	0.92	0.71	22.8

To further explore the relative elemental compositions changes of the CNT-based composites, EDS data were performed and listed in Table 1. It was clear that all the CNT-based composites contained C and O elements belonged to the pure CNT carrier. N element was also detected in the PANI/CNT composites and PANI/CNT-Pd catalysts, attributed to the characteristic elemental of PANI polymer. Meanwhile, S species were appeared in the PANI/CNT composites and PANI/CNT-Pd catalysts for the introduced -SO3H groups onto the CNT surface after diazotization[39]. Pd and Cl elements were found in the Pd-CNT and PANI/CNT-Pd catalysts, indicating that the Pd species were loaded on the carrier surface. Compared with the fresh Pd-based catalysts, the amount of the C and Cl element were increased but the relative Pd element content was decreased in the used Pd-CNT and 8PANI/CNT-Pd catalysts, which may be resulted from the carbon deposition generation and the loss of Pd and PANI species during the reaction[30]. From ICP results (Table 2), it was further confirmed that Pd species were lost in Pd-CNT and PANI/CNT-Pd catalysts during the reaction and Pd species loss is one reason for the decreasing of catalytic activity in Pd-based/CNT catalysts (Fig 4). Meanwhile, it was exhibited clearly that the loss ratio of Pd species in the 8PANI/CNT-Pd catalyst (22.8%) was much less than that in the Pd-CNT catalyst (50.6%), which suggested that the presence of the polyaniline layer in the Pd-based catalyst stabilize Pd species and retard Pd loss during the reaction, resulting the enhanced catalytic performance for acetylene hydrochlorination[30]. In addition, the N elements were decreased (about 9.39%) in

the used 8PANI/CNT-Pd catalyst after reaction (Table 1) and the decomposition of the polyaniline layer may be the possible reason decreased the catalyst activity (Fig 4).

Table 3. Porous structure parameters of the samples.

Sample	$S_{BET}/m^2 g^{-1}$	$V/cm^3 g^{-1}$	D/nm
CNT	133	0.16	2.69
8PANI/CNT	59	0.05	2.96
Fresh Pd-CNT	128	0.15	2.68
Used Pd-CNT	99	0.11	2.71
Fresh 8PANI/CNT-Pd	47	0.04	2.84
Used 8PANI/CNT-Pd	36	0.04	2.85

S_{BET}: surface area; V: total pore volume; D: average pore diameter.

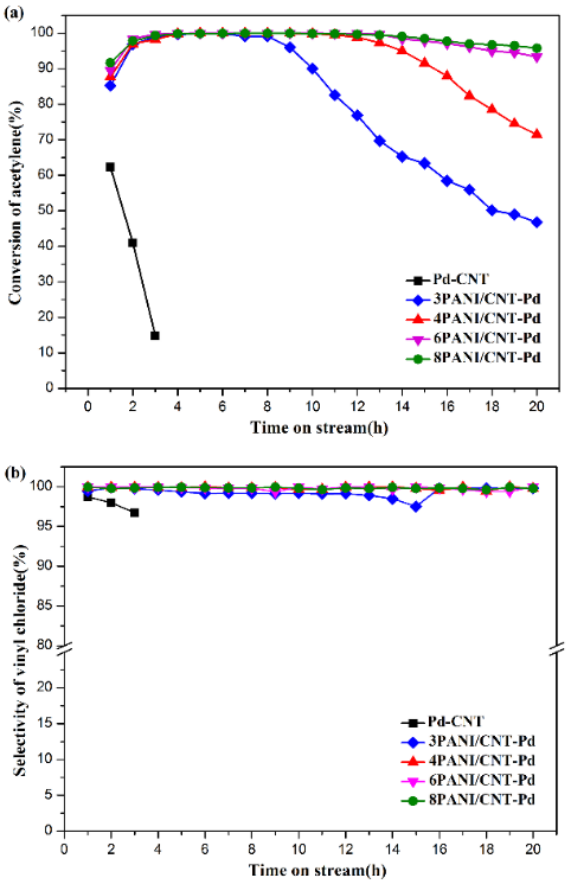

Fig.4. Catalytic performance of Pd-CNT and PANI/CNT-Pd catalysts. Reaction conditions: Temperature = 160 °C, C_2H_2 GHSV = 120 h^{-1}, feed volume ratio $V_{HCl}:V_{C2H2} = 1.5$.

BET analysis was performed and the surface area (SBET), total pore volume (V) and average pore diameter (D) of the pure CNT, the 8PANI/CNT composite and the fresh and used Pd-CNT and 8PANI/CNT-Pd catalysts were listed in Table 3. The untreated CNT has the highest surface area of 133 m2 g-1 and total pore volume of 0.16 cm3 g-1, whereas the CNT treated with PANI showed that the decrease of surface area and total pore size volume in the 8PANI/CNT composite. It was likely that the formation of PANI occupied portion of the CNT pore space resulted in a decrease surface area and total pore size volume, and this phenomenon could be observed from the morphologies of the PANI/CNT composites with various PANI contents in Fig 3. After Pd loading, the SBET and V were decreased but the D was increased in fresh Pd-based catalysts, resulted from the particle blocking of Pd species inside or outside the CNT-based carrier. After reaction, a lower SBET and V were observed and the D were increased in the used Pd-based catalysts attributed to the carbon deposition during the reaction[37], which was consistent with EDS results. Compared with the Pd-CNT catalyst, the 8PANI/CNT-Pd catalyst had less reduction changes of SBET and V, which may suggest that less carbon deposition occurred during the reaction.

The catalytic performance of Pd-CNT and the PANI/CNT-Pd catalysts were shown in Fig 4. It was clear that the acetylene conversion of Pd-CNT sharply decreased from 62.4% to 14.8% only after 3 h. This result proved that the unmodified Pd-CNT catalyst showed low acetylene conversion and stability. Contrary to the Pd-CNT catalyst, the PANI/CNT-Pd catalysts with a different mass of PANI modification exhibited excellent catalytic activity during acetylene hydrochlorination, which demonstrated that the polyaniline matrix serves to stabilize Pd-based catalysts. When the mass ratio of PANI was 80%, the 8PANI/CNT-Pd displayed the optimal catalytic performance (even though the 8PANI/CNT-Pd was on stream after 20 h, the acetylene conversion was above 91.6% and the vinyl chloride selectivity was above 99.6% all the time) under the reaction conditions in the acetylene hydrochlorination reaction. Moreover, the acetylene conversion was increased with the contents of PANI. It is likely that polyaniline can be coordinated to H2PdCl4 forming palladium complexes in the incipient wetness impregnation step of the catalyst preparation. That is to say Pd species were loaded on the CNT-based carrier through the introduction of PANI to bridge the Pd species and CNT walls with the presence of Pd-N bonding and π-π bonding, providing a better synergistic interaction[33-34,40]. So Pd species can be tightly anchored onto the CNT surface through Pd-N interactions with the N atoms of PANI and it seems that the plausible chelating effect between the nitrogen atom from PANI and the Pd species. It prevented Pd nanoparticles from aggregating with each other through polymeric stabilization, reduced the Pd species loss, and improved the long-term stability of the catalyst. Meanwhile, PANI species may be decomposed under reaction conditions (160 °C and the presence of HCl gas) and the polymeric stabilization was gradually weakening lead to Pd nanoparticles aggregating with each other. Thus, the polymeric stabilization may be increased with the contents of PANI during the reaction and prevented Pd nanoparticles from aggregating with each other and enhanced catalytic performance. In addition, the carbon deposition and Pd loss were also the main reasons for the decreases of the catalyst activity,30,31 which in agreement with the EDS (Table 1), ICP (Table 2) and BET results (Table 3).

4.Conclusions

In summary, Pd-PANI/CNT catalysts were prepared and displayed an excellent activity and stability (more than 91.6% acetylene conversion and 99.6% vinyl chloride selectivity in 20 h) under the conditions in the acetylene hydrochlorination reaction. It is suggested that PANI

species contained N elements have been deposited on the CNT surface and the presence of PANI has a significant influence on the catalytic activity and stability of CNT-based catalysts. This may be the existence of PANI (especially N species) to bridge the Pd species and CNT walls with the presence of Pd-N bonding and π-π bonding, which prevented Pd nanoparticles from aggregating with each other and Pd species loss, resulting in enhancing the catalytic performance. It was suggested that Pd species loss and the carbon deposition were the main reason for the PANI/CNT-Pd catalyst deactivation. In addition, it is suggested that the CNT can be a promising material to improve the catalytic performance of Pd-based catalysts for acetylene hydrochlorination reaction.

Acknowledgments

We gratefully acknowledge the financial support provided by the National Natural Science Foundation of China (No. 21968033 and No. U1903130), China Postdoctoral Foundation Program (2019M653800), Xinjiang Uygur Autonomous Region University Research program (XJEDU2018Y002), Doctoral Foundation of Xinjiang University (BS160222), Xinjiang Uygur Autonomous Region Graduate Student Innovation Project (XJ2019G050) and The program of introducing hundreds of young Doctors in Xinjiang Uygur Autonomous Region.

References

1. H. Xu, G. Luo, J. Ind. Eng. Chem. **5**, 13 (2018)
2. M. Zhu, Q. Wang, K. Chen, Y. Wang, C. Huang, H. Dai, F. Yu, L. Kang, B. Dai, ACS Catal. **5**, 5306 (2015)
3. G. Malta, S. A. Kondrat, S.J. Freakley, C.J. Davies, L. Lu, S. Dawson, A. Thetford, E. K. Gibson, D.J. Morgan, W. Jones, P.P. Wells, P. Johnston, C.R.A. Catlow, C.J. Kiely, G.J. Hutchings, Science. **355**, 1399 (2017)
4. P. Johnston, N. Carthey, G.J. Hutchings, J. Am. Chem. Soc. **137**, 14548 (2015)
5. S.A. Mitchenkoa, E.V. Khomutova, A.A. Shubinb, Y.M. Shul'ga, J. Mol. Catal. A-Chem. **212**, 345 (2004)
6. L. Wang, F. Wang, J. Wang. New J. Chem. **40**, 3019 (2016)
7. B. Man, H. Zhang, C. Zhang, X. Li, H. Dai, M. Zhu, B. Dai, J. Zhang, New J. Chem. **41**, 14675 (2017)
8. L. Wang, F. Wang, J. Wang, Catal. Commun. **83**, 9 (2016)
9. H. Zhang, B. Dai, W. Li, X. Wang, J. Zhang, M. Zhu, J. Gu, J. Catal. **316**, 141 (2014)
10. H. Zhang, B. Dai, X. Wang, L. Xu, M. Zhu, J. Ind. Eng. Chem. **18**, 49 (2012)
11. L. Ye, X. Duan, S. Wu, T. Wu, Y. Zhao, A.W. Robertson, H. Chou, J. Zheng, T. Ayvalı, S. Day, C. Tang, Y. Soo, Y. Yuan, S.C.E. Tsang, Nat. Commun. **10**, 914 (2019)
12. K. Zhou, W. Wang, Z. Zhao, G. Luo, J.T. Miller, M.S. Wong, F. Wei, ACS Catal. **4**, 3112 (2014)
13. W. Liu, M. Zhu and B. Dai, New J. Chem. **42**, 20131-20136. (2018)
14. J Zhao, B Wang. Y. Yue, G. Sheng, H. Lai, S. Wang, L. Yu, Q. Zhang, F. Feng, Z. Hu, X. Li, J. Catal. **373**, 240 (2019)
15. D. Hu, L. Wang, F. Wang, J. Wang, Chinese Chem. Lett. **29**,1413 (2018)
16. L. Wang, L. Lian, H. Yan, F. Wang, J. Wang, C. Yang, L. Ma, RSC Adv. **9**, 30335 (2019)
17. S. Shang, W. Zhao, Y. Wang, X. Li, J. Zhang, Y. Han, W. Li, ACS Catal. **7**, 3510 (2017)
18. Y. Yue, B. Wang, G. Sheng, H. Lai, S. Wang, Z. Chen, Z. Hu, J. Zhao, X. Li, New J. Chem. **43**, 12767 (2019)
19. J. Zhong, Y. Xu, Z. Liu, Green Chem. **20**, 1 (2018)
20. X. Tian, G. Hong, B. Jiang, F. Lu, Z. Liao, J. Wang, Y. Yang, RSC Adv. **5**, 46366 (2015)
21. L. Wang, F. Wang, J. Wang, Catal. Commun. **65**, 41 (2015)
22. J. Zhao, X. Cheng, L. Wang, R. Ren, J. Zeng, H. Yang, B. Shen, Catal. Lett. **144**, 2191 (2014)
23. X. Li, X. Pan, L. Yu, P. Ren, X. Wu, L. Sun, F. Jiao, X. Bao, Nat. Commun. **5**, 3688 (2014)
24. P. Serp, M. Corrias, P. Kalck, Appl. Catal. A-Gen. **253**, 337 (2013)
25. R.H. Baughman, A.A. Zakhidov, W.A. Heerde, Science. **297**, 787 (2002)
26. B. Wu, Y. Kuang, X. Zhang, J. Chen, Nano Today. **6**, 75 (2011)
27. X. Li, X. Pan, X. Bao B, J. Energy Chem. **23**,131 (2014)
28. K. Zhou, J. Jia, C. Li, H. Xu, J. Zhou, G. Luo, F. Wei, RSC Adv. **4**,7766 (2014)
29. K. Zhou, B. Li, Q. Zhang, J. Huang, G. Tian, J. Jia, M. Zhao, G. Luo, D. Su, F. Wei, ChemSusChem. **7**, 723 (2014)
30. L. Wang, F. Wang, J. Wang, Catal. Commun. **74**, 55 (2016)
31. X. Li, M. Zhu, B. Dai, Appl. Catal. B-Environ. **142-143**, 234 (2013)
32. R. Lin, S.K. Kaiser, R. Hauert, J. Pérez-Ramírez. ACS Catal. **8**, 1114 (2018)
33. F. Wang, L. Wang, J. Wang, React. Kinet. Mech. Cat. **114**, 725 (2015)
34. J. Chen, W. Zhang, L. Chen, L. Ma, Chempluschem. **78**, 142 (2013)
35. S.I.A. Razak, A.L. Ahmad, S.H.S. Zein, A.R. Boccaccini, Scripta. Mater. **61**, 592 (2009)
36. M. Cao, J. Yang, W. Song, D. Zhang, B. Wen, H. Jin, Z. Hou, J. Yuan, ACS Appl. Mater. Inter. 4, 6949 (2012)
37. T. Wu, Y Lin. Polymer. **47**, 3576 (2006)
38. G. Nie, X. Tong, Y. Zhang, M. Liang, X. Zhuang, S. Xue. Res. Chem. Intermediat. 42, 8305 (2016)

39. Z. Zhu, G. Wang, M. Sun, X. Li, C. Li, Electrochim. Acta. **56**, 1366. (2011)
40. S. Giri, D. Ghosh, A. Malas, C.K. Das, J. Electron. Mater. **42**, 2595 (2013)